J|A|C|S
ARTICLES
Published on Web 11/15/2002

Hybridization of Mismatched or Partially Matched DNA at Surfaces

Alexander W. Peterson, Lauren K. Wolf, and Rosina M. Georgiadis*

Contribution from the Department of Chemistry, Boston University, Metcalf Center for Science and Engineering, Boston Massachusetts 02215

Received August 3, 2002

Abstract: We investigate how probe density influences hybridization for unlabeled target oligonucleotides that contain mismatched sequences or targets that access different binding locations on the immobilized probe. We find strong probe density effects influencing not only the efficiency of hybridization but also the kinetics of capture. Probe surfaces are used repeatedly, and the potentially large contributions of sample-to-sample variations in surface heterogeneity and nonspecific adsorption are addressed. Results of kinetic, equilibrium, and temperature-dependent studies, obtained using in-situ surface plasmon resonance (SPR) spectroscopy, show that hybridization for surface immobilized DNA is quite different from the well-studied solution-phase reaction. Surface hybridization depends strongly on the target sequence and probe density. Much of the data can be explained by the presence of steric crowding at high probe density; however, the behavior of mismatched sequences cannot be understood using standard models of hybridization even at the lowest density studied. In addition to unusual capture kinetics observed for the mismatched targets, we find that the binding isotherms can be fit only if a heterogeneous model is used. For mismatched targets, the Sips model adequately describes probe-target binding isotherms; for perfectly matched targets, the Langmuir model can be used.

Introduction

Hybridization of surface immobilized DNA is increasingly important in both fundamental and applied research in chemistry, biology, and nanoscience. For example, widely used microarray-based techniques for DNA variation analysis involve hybridization of immobilized oligonucleotide probe strands with solution-phase targets.[1−6] In nanoscience applications, oligonucleotides can be used to arrange, on the nanoscale, the materials to which they are attached.[7−12]

Fundamentally, all of these applications rely on the specificity or stringency of hybridization, the process by which single-stranded DNA (ssDNA) oligonucleotides form stable duplexes or hybrids. The factors that control hybridization have been extensively investigated for solution-phase DNA, especially for perfectly matched strands and, more recently, for mismatched DNA.[13] In contrast, fewer investigations have focused on the in-situ kinetics and thermodynamics for surface immobilized probes interacting with solution-phase targets, where the molecular level processes are more complex. These processes involve additional factors that are much less well understood, such as probe density, surface heterogeneity and nonspecific adsorption. The importance of such complex factors is increasingly recognized but remains largely unaddressed in published experiments. For example, probe density dependent kinetic or steric constraints may alter the apparent stability or selectivity of probe-target binding for surface immobilized oligonucleotides. These effects are particularly difficult to investigate for short oligonucleotide probes produced by light directed synthesis, where a distribution of strand lengths and sequences is produced.[14] Even when pre-fabricated oligonucleotide probes of known sequence and length are attached to a surface, the surface probe density (number of probes per unit area) is often not reported because quantitation of unlabeled probes is difficult.[6,15] Some studies, aimed to alleviate steric effects, have used oligonucleotide surface spacers to move probes away from

* To whom correspondence should be addressed. E-mail: rgeorgia@bu.edu.

(1) Lockhart, D. J.; Dong, H. L.; Byrne, M. C.; Follettie, M. T.; Gallo, M. V.; Chee, M. S.; Mittmann, M.; Wang, C. W.; Kobayashi, M.; Horton, H.; Brown, E. L. *Nat. Biotechnol.* **1996**, *14*, 1675−1680.
(2) Southern, E.; Mir, K.; Shchepinov, M. *Nature Genet.* **1999**, *21*, 5−9.
(3) Mir, K. U.; Southern, E. M. *Nat. Biotechnol.* **1999**, *17*, 788−792.
(4) Tillib, S. V.; Mirzabekov, A. *Curr. Opin. Biotechnol.* **2001**, *12*, 53−58.
(5) Lipshutz, R. J.; Fodor, S. P. A.; Gingeras, T. R.; Lockhart, D. J. *Nature Genet.* **1999**, *21*, 20−24.
(6) Hughes, T. R.; Mao, M.; Jones, A. R.; Burchard, J.; Marton, M. J.; Shannon, K. W.; Lefkowitz, S. M.; Ziman, M.; Schelter, J. M.; Meyer, M. R.; Kobayashi, S.; Davis, C.; Dai, H. Y.; He, Y. D. D.; Stephaniants, S. B.; Cavet, G.; Walker, W. L.; West, A.; Coffey, E.; Shoemaker, D. D.; Stoughton, R.; Blanchard, A. P.; Friend, S. H.; Linsley, P. S. *Nat. Biotechnol.* **2001**, *19*, 342−347.
(7) Mirkin, C. A.; Letsinger, R. L.; Mucic, R. C.; Storhoff, J. J. *Nature* **1996**, *382*, 607−609.
(8) Alivisatos, A. P.; Johnsson, K. P.; Peng, X. G.; Wilson, T. E.; Loweth, C. J.; Bruchez, M. P.; Schultz, P. G. *Nature* **1996**, *382*, 609−611.
(9) Winfree, E.; Liu, F. R.; Wenzler, L. A.; Seeman, N. C. *Nature* **1998**, *394*, 539−544.
(10) Park, S. J.; Lazarides, A. A.; Mirkin, C. A.; Letsinger, R. L. *Angew. Chem.-Int. Edit.* **2001**, *40*, 2909−2912.
(11) Seeman, N. C. *Nano Lett.* **2001**, *1*, 22−26.
(12) Gerion, D.; Parak, W. J.; Williams, S. C.; Zanchet, D.; Micheel, C. M.; Alivisatos, A. P. *J. Am. Chem. Soc.* **2002**, *124*, 7070−7074.
(13) Bloomfield, V. A.; Crothers, D. M.; Tinoco, I. *Nucleic Acids Structures, Properties, and Functions*; University Science Books: Sausalito, 2000.
(14) Forman, J. E.; Walton, I. D.; Stern, D.; Rava, R. P.; Trulson, M. O. In *Molecular Modeling of Nucleic Acids*; AMER CHEMICAL SOC: Washington, 1998; Vol. 682, pp 206−228.
(15) Liebermann, T.; Knoll, W.; Sluka, P.; Herrmann, R. *Colloid Surf. A-Physicochem. Eng. Asp.* **2000**, *169*, 337−350.

Table 1. Oligonucleotide Sequences and Nomenclature

probe: 25 thiol	HS−C_6−5′- AGATCAGTGCGTCTGTACTAGCACA-3′
target: PM	3′- TCTAGTCACGCAGACATGATCGTGT-5′
target: 2MM	3′- TCTAGTCACACAGACATCATCGTGT-5′
target: 1MM	3′- TCTAGTCACĀCAGACATGATCGTGT-5′
target: 18 high	3′- ACGCAGACATGATCGTGT-5′
target: 18 low	3′- TCTAGTCACGCAGACATG-5′
target: 25 control	3′- ACACGATCATGTCTGCGTGACTAGA-5′

Scheme 1. Diagram of the Immobilization Strategy that Uses an Immobilized 25-mer Probe (fixed sequence) and Five Different Target Oligonucleotides

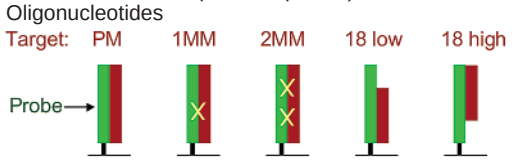

the surface and enhance hybridization,[16,17] but probe density is not controlled. Even when probe densities are reported, the extent of hybridization is considered[16,18] but not the rate of capture.

The properties of mismatched (MM) oligonucleotides, which are less understood than those of perfectly matched (PM) oligonucleotides, are important for various applications including the technology for detecting single nucleotide polymorphisms across the genome. In the identification of genes using some photolithographically synthesized oligonucleotide microarrays,[5] the response from PM and MM probes is compared. Although this approach has been suggested[14] as a means of reducing artifacts such as contributions from nonspecific binding, no published experimental data establishes the assumptions of this approach.[19] Contrary to expectation, recent statistical analyses find large fractions of MM probes exhibiting higher signal levels than the corresponding PM probes. This behavior suggests that hybridization on microarrays is more complex than expected and raises the possibility that fluorescence labeling may play a role.[20]

Initial work from our laboratory showed that the kinetics of hybridization for unlabeled DNA oligonucleotides are extremely sensitive, not only to the presence of mismatch base-pairs, but also to the position of hybridization relative to the surface.[21] We suggested that lateral interactions with nearby probe DNA molecules could affect the kinetics. A subsequent study on perfectly matched DNA, in which the probe density was varied by an order of magnitude, confirmed that both the rate of target capture and the extent of hybridization depend strongly on surface probe density.[22]

Here, we examine five different solution-phase target oligonucleotides, Table 1, interacting with the same tethered probe oligonucleotide, Scheme 1. The oligonucleotide targets include two thermodynamically equivalent 18-mer strands that bind to

Scheme 2. Illustration of Probe Densities Used in This Work.

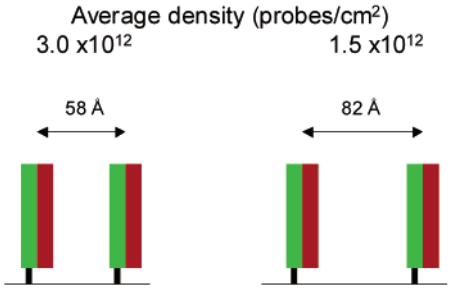

At the higher density, the orientation of duplexes is preferentially oriented toward the surface normal (ref 25); at the lower probe density, the orientation is not known.

different locations on the 25-mer probe strand and a series of three 25-mer strands that contain increasing mismatch content, including a single base-pair mismatch. Circular dichroism and UV−vis melting experiments confirm that thermodynamic differences between these targets in solution are in reasonable agreement with calculations.[23,24] Both 18-mer targets form solution duplexes that have melting transition temperatures ∼6 °C lower than the PM duplex, whereas 1MM and 2MM targets have melting temperatures ∼5 °C and ∼10 °C lower than the PM target.

We investigate these probe-target interactions at two different probe densities, Scheme 2. For the denser film, inter-probe interactions or cross hybridization of targets may come into play.[25] Indeed, Levicky et al. concluded that lateral interactions among neighboring surface hybrids on a film of similar density led to an upright orientation measured via thickness determination in neutron reflectivity studies.[26] At the second, lower, density studied here, such steric effects should be minimized because of the larger probe-probe separation, approximately equal to the calculated[27] duplex length.

We use surface plasmon resonance spectroscopy (SPRS) to monitor the kinetics of hybridization and to quantitatively characterize the surface probe density, as well as determine capture efficiencies and probe-target binding constants. This optical technique, which does not require fluorescent probes or other labels, has been used previously in our laboratory to study the kinetics and thermodynamics of DNA monolayer films.[21,28−30] Preparation of the probe film involves the attachment of a thiolated DNA 25-mer oligonucleotide to the SPR sensor surface via a covalent gold-thiol bond. Controlling the exposure time and concentration of the probe solution attains the desired probe

(16) Guo, Z.; Guilfoyle, R. A.; Thiel, A. J.; Wang, R. F.; Smith, L. M. *Nucleic Acids Res.* **1994**, *22*, 5456−5465.
(17) Shchepinov, M. S.; CaseGreen, S. C.; Southern, E. M. *Nucleic Acids Res.* **1997**, *25*, 1155−1161.
(18) Steel, A. B.; Herne, T. M.; Tarlov, M. J. *Anal. Chem.* **1998**, *70*, 4670−4677.
(19) Chudin, E.; Walker, R.; Kosaka, A.; Wu, S. X.; Rabert, D.; Chang, T. K.; Kreder, D. E. *Genome Biol* **2001**, *3*, 5000−5010.
(20) Naef, F.; Lim, D. A.; Patil, N.; Magnasco, M. *Phys. Rev. E* **2002**, *65*, 040901−040904.
(21) Peterson, A. W.; Heaton, R. J.; Georgiadis, R. *J. Am. Chem. Soc.* **2000**, *122*, 7837−7838.
(22) Peterson, A. W.; Heaton, R. J.; Georgiadis, R. M. *Nucleic Acids Res.* **2001**, *29*, 5163−5168.
(23) SantaLucia, J. *Proc. Natl. Acad. Sci. U.S.A.* **1998**, *95*, 1460−1465.
(24) Peyret, N.; Seneviratne, P. A.; Allawi, H. T.; SantaLucia, J. *Biochem.* **1999**, *38*, 3468−3477.
(25) For the higher probe density (3.0×10^{12} probes/cm^2), we expect a film composed of rigid DNA cylinders spaced center-to-center as shown in Scheme 2, which adopt a preferential orientation toward the surface normal. This structure is based on neutron reflectivity studies, ref 26, for perfectly matched 25-mer duplexes which find an average tilt angle of ∼30° from the surface normal for a density of 3.0×10^{12} probes/cm^2 and a volume fraction of 7%. On the basis of solution-phase data, the diameter of each cylinder is expected to be ∼20 Å for duplex DNA; a concentric sheath of condensed counterions would increase the effective diameter slightly at the high solution ionic strength (1M) used.
(26) Levicky, R.; Herne, T. M.; Tarlov, M. J.; Satija, S. K. *J. Am. Chem. Soc.* **1998**, *120*, 9787−9792.
(27) Mathews, C. K.; van Holde, K. E. *Biochemistry*; Benjamin/Cummings: Redwood City, 1990.
(28) Peterlinz, K. A.; Georgiadis, R. *Opt. Commun.* **1996**, *130*, 260−266.
(29) Georgiadis, R.; Peterlinz, K. P.; Peterson, A. W. *J. Am. Chem. Soc.* **2000**, *122*, 3166−3173.
(30) Heaton, R. J.; Peterson, A. W.; Georgiadis, R. M. *Proc. Natl. Acad. Sci. U.S.A.* **2001**, *98*, 3701−3704.

density.[22] This fabrication method has been shown previously to result in robust, reusable DNA probe films which show reproducible rates and efficiencies of target capture, provided that films of the same probe density are compared.[22] Nonspecific adsorption is eliminated by the use of mercaptohexanol as a component in the monolayer film.

The probe densities used in this work are a small percentage (<10% monolayer) of a theoretical fully packed DNA monolayer film and in the same range as many published applications that exploit DNA hybridization.[18,31] Detection of hybridization is feasible at much lower probe densities with the addition of fluorescent labels. Nevertheless, for commonly used fluorescent microarrays, the number of active probes per unit area appears comparable to the range used here.[14]

This is the first systematic study to examine the effects of probe density on both the kinetics and absolute binding efficiencies of a series of well-characterized, prefabricated oligonucleotide targets of selected sequence and length. An important feature of this work is that results are highly reproducible so that the same probe surface is reused repeatedly. Therefore, comparisons involving different target sequences can be made without concerns about sample-to-sample variations in surface heterogeneity or nonspecific binding. Careful analysis of binding isotherms and kinetic data reveal that the behavior of MM targets cannot be understood on the basis of simple models of hybridization. This type of approach is needed to gain insight into how interfacial hybridization may differ from solution-phase duplex formation and provides valuable information, often not obtained by other methods, important for many different applications of immobilized DNA on solid supports.

Experimental Methods

Oligonucleotide Sequences. Table 1 identifies the oligonucleotides used in these experiments. The HPLC purified oligonucleotide probe, functionalized at the 5′ end with a thiol group connected by a hexamethylene linker ($HS-C_6$-ssDNA), was obtained from Integrated DNA Technologies. The HPLC purified oligonucleotide targets were obtained from Alpha DNA.

Immobilization Procedure. Scheme 1 shows the immobilization strategy and probe-target binding schematic in which the same immobilized probe sequence is used with five different targets; Scheme 2 depicts the probe densities used in this work. Probe films were fabricated following the sequential immobilization procedures used earlier.[29] To achieve a final probe density of 3.0×10^{12} probes/cm^2, the gold substrate was exposed to a 1 μM solution of thiolated DNA probe strand for ~120 min. The 1.5×10^{12} probes/cm^2 film was produced by substrate exposure to 0.1 μM thiolated probe solution for ~30 min. After probe immobilization, DNA films were treated with 1mM mercaptohexanol (MCH) solution for 1−2 h. The mixed film was then heated in water to at least 60 °C before hybridization experiments were performed. Prior to probe immobilization, the gold substrate was cleaned with piranha solution [7:3 mixture of H_2SO_4 (EM Science) and H_2O_2 (Mallinckrodt)].

As described previously,[29] the SPR response was used to monitor probe density during initial DNA thiol immobilization and to quantify any losses in subsequent steps due to rinsing with buffer or DNA probe displacement by MCH. Typically, DNA probe rinsing losses after the initial immobilization are highly dependent on the film density and can vary from ~0% for the highest density films to ~60% loss for very low-density films.

Hybridization Procedure. For hybridization kinetics experiments, the probe film was exposed to the hybridization buffer containing 1 μM target for at least 10 h in a static cell. A control experiment, using a noncomplementary target solution (25 control), confirmed that nonspecific binding was completely absent, in agreement with previous observations for higher density probe films.[32]

For binding constant measurements in which a probe film was exposed to a series of concentrations of the same target, experiments were performed until steady-state hybridization was reached under flow conditions (~0.2 mL/sec for 7 mL total volume). Target concentrations in the range 2−400 nM were used in addition to 1 μM.

For hybridization equilibrium measurements in which films undergo mild heating, the probe film was first exposed to the target hybridization buffer for 10+ hours at room temperature. Equilibrium SPR measurements were then taken. During mild heating, the target hybridization buffer, still in contact with the probe film, was heated to 37 °C and cooled back to room temperature over a time period of 3+ h. SPR measurements were then performed at room temperature.

Regeneration of Probe Films. For each probe density, repeated measurements were performed on the same DNA film. Regeneration of the single-stranded probe film after hybridization experiments was achieved by denaturation of the surface duplex by rinsing with hot water (>60 °C). Highly reproducible behavior is observed for probe films generated on different gold substrates provided that the probe density is identical.

Preparation of Solutions. All solutions were prepared with 18 MΩ/cm purified water from a Barnstead E-pure system. For immobilization of DNA thiols, solutions were prepared as 1μM 25 thiol (or 0.1 μM 25 thiol for the lowest density probe surface) in 1M KH_2PO_4 (Sigma). Mercaptohexanol (Aldrich) was prepared as a 1mM solution in water. Hybridization solutions were prepared as 1 μM target in 1M NaCl containing TE buffer (10mM Tris buffer (pH 7.6) and 1mM EDTA) (All Sigma−SigmaUltra Grade).

SPR Measurements. The two-color SPR apparatus setup and procedure for analysis of measurements have been described previously[28,33] as have details of how quantitative measurements of coverage are extracted from raw SPR reflectance data. Briefly, the SPR reflectance data was analyzed by fitting the data to a multilayer Fresnel model to extract the thickness and dielectric constant of the unknown DNA layer. The resulting best-fit parameters were converted to coverage of DNA (in molecules/cm^2) as outlined previously.[29,32] Hybridization efficiency was calculated by dividing the hybridized target coverage by the immobilized probe coverage. As in previous work, these calculations assumed an equivalent SPR response per unit coverage for single-stranded DNA oligonucleotides at the SPR surface regardless of whether the DNA consisted of surface-immobilized probes or targets undergoing surface hybridization. Good agreement has been reported[18,34,35] between our SPR results and the results of radiolabeling, fluorescence, and quantitative electrochemistry studies.

Consequences of Assuming an Isotropic Refractive Index for DNA. It is well-known that the refractive index, n, or dielectric constant, $\epsilon = n^2$, of DNA is anisotropic due to π electrons in the bases.[36,37] However, our SPR analysis assumes the DNA layer to be homogeneous or isotropic[29,32] both for ssDNA, which has a very short persistence length and therefore might be expected to show a homogeneous response, and duplex DNA which, for the strand lengths used here, is expected to be a rigid rod. Neutron reflectivity studies on oligonucleotides of the same length show that duplex DNA films at similar coverage

(31) Demers, L. M.; Mirkin, C. A.; Mucic, R. C.; Reynolds, R. A.; Letsinger, R. L.; Elghanian, R.; Viswanadham, G. *Anal. Chem.* **2000**, *72*, 5535−5541.
(32) Peterlinz, K. A.; Georgiadis, R. M. *J. Am. Chem. Soc.* **1997**, *119*, 3401−3402.
(33) Peterlinz, K. A.; Georgiadis, R. *Langmuir* **1996**, *12*, 4731−4740.
(34) Mbindyo, J. K. N.; Reiss, B. D.; Martin, B. R.; Keating, C. D.; Natan, M. J.; Mallouk, T. E. *Adv. Mater.* **2001**, *13*, 249−254.
(35) Herne, T. M.; Tarlov, M. J. *J. Am. Chem. Soc.* **1997**, *119*, 8916−8920.
(36) Caspersson, T. *Nature* **1938**, *141*, 122−122.
(37) Wilkins, M. H. F.; Gosling, R. G.; Seeds, W. E. *Nature* **1951**, *167*, 759−760.

to our higher density film, are preferentially ordered toward the surface normal;[26] however, no information is available for the orientation of DNA as a function of coverage, which may effect the duplex orientation. Therefore, we might expect some error associated with assuming a single isotropic refractive index in the analysis of data involving ssDNA and dsDNA regardless of coverage. Of course, any refractive index anisotropy would be mediated by surface roughness because the SPR substrates consist of evaporated gold on glass, which are far from atomically flat surfaces. Nevertheless, we examine the consequences of assuming an isotropic refractive index on the coverage (number of DNA molecules per unit area) and hybridization efficiencies reported.

In our analysis of SPR reflectance curves, in terms of a multilayer Fresnel reflectivity model, we treat the DNA as a homogeneous layer using values for the DNA component estimated or calculated as described earlier.[29,32] These are as follows: the isotropic dielectric constant, $\epsilon_{DNA} = 2.5$, the refractive index increment, $\Delta n/\Delta c = 0.14$ cm^3/g, where c is the concentration of DNA, and the density, $\rho = 1.63$ g/cm^3. These values are in good agreement with data reported by Lindsay and co-workers,[38] $\Delta n/\Delta c = 0.163$ cm^3/g and $\rho = 1.64$ g/cm^3. However, in that study on wet-spun films of DNA, the authors report an anisotropy of $\Delta\epsilon = \epsilon_{||} - \epsilon_{\perp} \approx 0.1$, for the dielectric constant perpendicular and parallel to the duplex helix axis.[38]

On the basis of this information, we can set an upper limit on the error associated with the anisotropy in the optical properties of DNA. If we considered two films containing the same number of DNA molecules, one in which 100% of the molecules were oriented upright and another where 100% were laying flat along the surface, the latter film would show a larger SPR response (larger angle shift). However, at the extremely low densities in this work (volume fraction of DNA <10%) there would be, at most, an error of 12−15% in the deduced coverage. Because the refractive index of ssDNA is likely to lie between $\epsilon_{||}$ and $\epsilon_{\perp}$, we would expect even smaller errors in the hybridization efficiency calculations. In this paper, we make no assumptions about the orientation of DNA and use an isotropic refractive index. At the low DNA coverages used here, the largest possible effect of anisotropy in the refractive index of DNA is not significant relative to the noise; therefore, the use of an isotropic refractive index in the calculation of DNA coverage does not alter the conclusions of this paper.

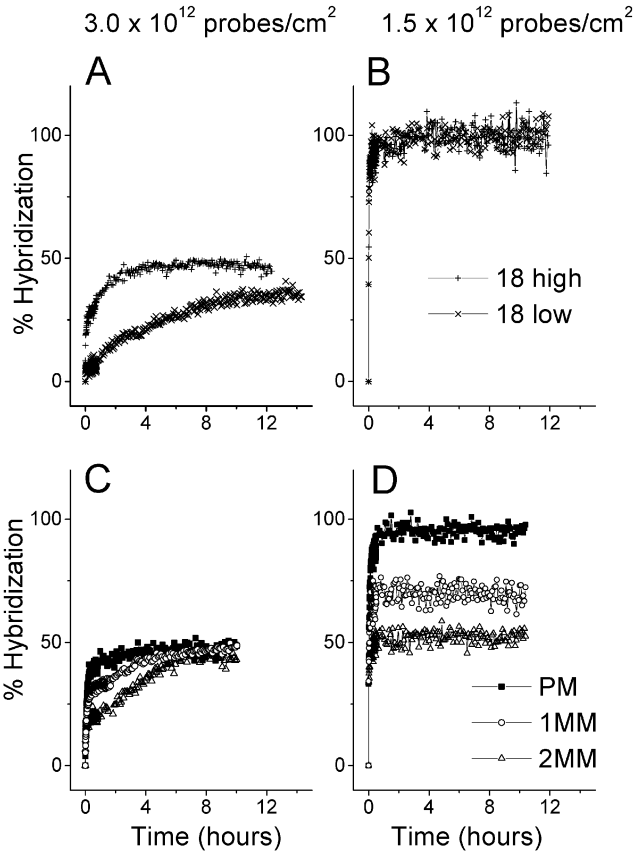

Figure 1. Comparison of hybridization kinetics for five different target strands onto probe films of two different surface densities. Hybridization conditions are 1 μM target concentration and high solution ionic strength (1M NaCl). The top graphs, (A and B), show capture kinetics for 18 high and 18 low targets; the bottom graphs, (C and D), show PM, 1MM, and 2MM targets. The probe density is 3.0×10^{12} probes/cm^2 (left, A and C) and 1.5×10^{12} probes/cm^2 (right, B and D). At each probe density, all five targets are hybridized repeatedly onto the same probe film. Nonspecific binding is negligible for the 25-control target.

Results and Discussion

Kinetics. For oligonucleotide strands of short lengths, a commonly accepted model for duplex formation is that of nucleation followed by helix zipping.[39,40] In this picture, mismatches near the middle of a strand are not expected to change the rate of duplex formation, but rather would affect the rate for the reverse process and, of course, the equilibrium binding constant $K_A = k_{on}/k_{off}$. All else being equal, the position of hybridization along the strand (distance from the surface) is expected to affect the efficiency or rate of duplex formation if nucleotides near the surface are less accessible as nucleation sites, particularly under high probe density conditions. To investigate the effects of mismatch and hybridization position, we studied five different partially matched and mismatched targets, and compared their hybridization behaviors at two different probe densities (Figure 1).

We consider first only the perfectly matched target sequences (25 PM, 18 high, 18 low). All of the results for these sequences, including striking differences in kinetics and efficiency, can be explained with a simple physical picture of interfacial hybridization that incorporates steric hindrance at high probe density. At the higher density studied here (3.0×10^{12} probes/cm^2), the kinetics of hybridization for the perfect match (Figure 1C, ■) and 18 high (Figure 1A, +) targets are similarly slow, requiring several hours to reach steady-state hybridization. Even after many hours, saturation does not exceed ~50% overall efficiency. In contrast, the 18 low target (Figure 1A, ×), which must hybridize closer to the surface, shows dramatically slower kinetics, requiring over 14 h to reach the same efficiency. Presumably, the target must penetrate further into the DNA film before nucleation and zipping can occur since the seven distal probe nucleotides are noncomplementary to this target.

When the probe density is reduced to 1.5×10^{12} probes/cm^2, the results are dramatically different. First, the kinetics become much more rapid, approaching Langmuir[41] behavior. Second, the hybridization efficiency reaches 100% within ~1 h. Finally, hybridization at the proximal end (required for 18 low targets) vs the distal end of the immobilized strand (available to the 18 high and 25 PM) is now indistinguishable. Turning now to mismatched sequences and comparing targets with a fully complementary sequence (25 PM), a single base-

(38) Weidlich, T.; Lindsay, S. M.; Rupprecht, A. *Biopolymers* **1987**, *26*, 439−453.
(39) Craig, M. E.; Crothers, D. M.; Doty, P. *J. Mol. Bio.* **1971**, *62*, 383−401.
(40) Cantor, C. R.; Schimmel, P. *Biophysical Chemistry, Part I*; WH Freeman: New York, 1980.

(41) The steady state for each target is reached rather quickly (<1/2 h) and remains constant for many hours. Careful fitting (not shown) at short times (<1/2 h) indicates that a first-order Langmuir model cannot sufficiently describe the kinetics.

pair mismatch (1MM), and a two base-pair mismatch (2MM), we find that the capture efficiencies and kinetics of hybridization are harder to understand considering only steric crowding. At the higher density, 3.0×10^{12} probes/cm^2, introduction of even one mismatch dramatically alters the kinetics of hybridization. However, the behavior here is complex in that more than a single process is evident and saturation is extremely slow, but reproducible. Despite differences in kinetics, an overall hybridization efficiency of ~50% is eventually attained. This efficiency is generally consistent with that seen for perfectly matched targets, in that about 50% of the immobilized probe sites at this density appear to be inaccessible because of steric crowding. Kinetic differences in PM and MM target hybridization have been previously reported by our laboratory[21,30] and others.[42,43] However, it is not clear how mismatches near the middle of the strand have such strong effects on hybridization.

When the probe density is reduced to 1.5×10^{12} probes/cm^2, the rates of target capture increase as expected. All three kinetic isotherms appear more Langmuir-like;[41] however, the maximum hybridization efficiencies do not reach the expected 100% level except for the PM target. The others remain limited to 70% for 1MM, and 50% for 2MM. Thus, even though 100% of the probes are available for binding at this density, a smaller percentage is achieved when mismatched targets are used.

Although there are few experiments involving immobilized DNA to which comparisons can be made, recent work performed at room temperature for DNA immobilized at cantilever surfaces provides some information.[43−45] Majumdar and coworkers[43] observe differences in cantilever deflection for both terminal and internal mismatches. For short 10-mer sequences, a reversal of cantilever deflection was observed only for internally mismatched targets in contrast to positive deflection for PM targets. Unhybridized mismatched regions or dangling target ends most likely increase the surface configurational entropy, causing the unexpected deflection. Although probe density effects were not considered, these studies suggest the existence of a hybridization barrier for internal mismatch sequences, in general agreement with our observations of reduced hybridization efficiency for mismatched targets.

In many studies involving immobilized probes of short length, mismatch discrimination can be achieved by simply rinsing with buffer, which leads to preferential loss of the less stable targets. In this work, mismatch discrimination is observed in-situ at high ionic strength (1 M) and high target concentration (1 μM) conditions that strongly favor duplex formation. Under these conditions, others observe single nucleotide discrimination for internal mismatches[46] with relatively short oligonucleotides (<15mer)[14,16] but not with longer strands; for example no discrimination is observed with 20-mer oligonucleotides.[14] Given the relatively small thermodynamic differences arising from 1 or 2 mismatches out of 25 base-pairs, we expect MM targets to reach 100% hybridization efficiency at room temperature and saturating solution concentrations. Clearly, this is not observed and it appears that there is a barrier preventing the mismatched targets from reaching higher binding efficiency.

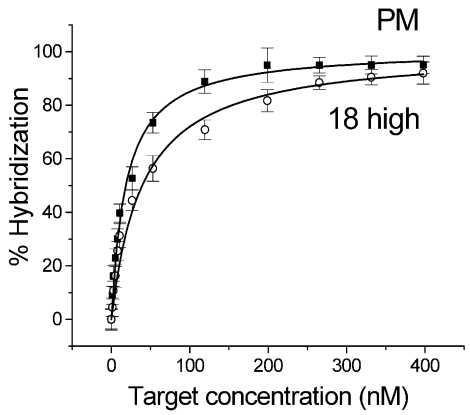

Figure 2. Equilibrium isotherms for hybridization of PM (■) and 18 high (○) targets measured on the same probe film (1.5×10^{12} probes/cm^2). Steady state hybridization efficiencies are measured sequentially on the same probe film after the target coverage reaches saturation at the solution concentrations shown. Langmuir fits (solid lines) to each equilibrium isotherm with $\Gamma_{max} = 100\%$, yield binding constants, K_A, equal to 6×10^7 M^{-1} and 3×10^7 M^{-1} for PM and 18 high, respectively. For both isotherms, data at 1 μM target concentration (not shown) is included in the fitting analysis. Error bars reflect the averaged SPR signal over a 15 min period after equilibrium is reached and are related to thermal noise.

Equilibrium Binding Isotherms at Low Probe Density. Further understanding of hybridization interactions can be elucidated from measurements of duplex thermodynamic stability. This can be achieved by a number of methods including in-situ melting, which has been reported for unlabeled oligonucleotides at higher densities[21,32] and for fluorescently labeled targets.[14,47] However, experimental and interpretational difficulties can limit the utility of temperature dependent measurements. Alternatively, equilibrium binding constants can be determined from isotherms. In this section, we study binding isotherm data obtained sequentially on the same probe film of density 1.5×10^{12} probes/cm^2.

For perfectly matched DNA, interpretation of binding isotherm data, Figure 2, on the basis of a simple Langmuir model, leads to the reasonable conclusion that the 18-mer target duplex is less stable than the 25-mer target duplex on the same immobilized probe surface. The equilibrium constants, K_A, are found to be 6×10^7 M^{-1} and 3×10^7 M^{-1} for PM and 18 high, respectively.

Our SPR measurements, even at these very low probe densities, are sensitive enough to detect differences in binding energies between 18-mer and 25-mer targets. This appears as a difference in the curvature in Figure 2. In contrast, we do not observe this expected behavior for mismatched targets, which also form duplexes that are thermodynamically less stable than the PM hybrid; rather, the saturation level seems to decrease, as in Figure 3.

A cursory analysis of the mismatched DNA binding isotherms in Figure 3, using the Langmuir model, could lead to the erroneous conclusion that there is no difference in the binding constant for matched and mismatched duplexes. A more careful analysis of the data, discussed further below, reveals that application of the Langmuir model is not justified in the case

(42) Hook, F.; Ray, A.; Norden, B.; Kasemo, B. *Langmuir* **2001**, *17*, 8305−8312.
(43) Hansen, K. M.; Ji, H. F.; Wu, G. H.; Datar, R.; Cote, R.; Majumdar, A.; Thundat, T. *Anal. Chem.* **2001**, *73*, 1567−1571.
(44) Fritz, J.; Baller, M. K.; Lang, H. P.; Rothuizen, H.; Vettiger, P.; Meyer, E.; Guntherodt, H. J.; Gerber, C.; Gimzewski, J. K. *Science* **2000**, *288*, 316−318.
(45) Wu, G. H.; Ji, H. F.; Hansen, K.; Thundat, T.; Datar, R.; Cote, R.; Hagan, M. F.; Chakraborty, A. K.; Majumdar, A. *Proc. Natl. Acad. Sci. U.S.A.* **2001**, *98*, 1560−1564.
(46) Pease, A. C.; Solas, D.; Sullivan, E. J.; Cronin, M. T.; Holmes, C. P.; Fodor, S. P. A. *Proc. Natl. Acad. Sci. U.S.A.* **1994**, *91*, 5022−5026.
(47) Watterson, J. H.; Piunno, P. A. E.; Wust, C. C.; Krull, U. J. *Langmuir* **2000**, *16*, 4984−4992.

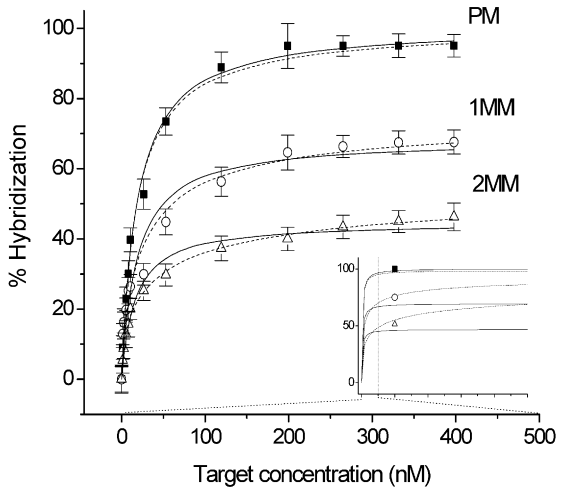

Figure 3. Equilibrium isotherms for hybridization of PM, 1MM and 2MM targets, measured on the same probe film, density = 1.5×10^{12} probes/cm^2, and comparison with adsorption models. Using the Langmuir model (solid line), the binding constant is determined to be the same for all three targets, $K_A \approx 6 \times 10^7$ M^{-1}, whereas for the Sips model (dashed line), $K_A = 6 \times 10^7$ M^{-1}, 1×10^7 M^{-1} and 2×10^6 M^{-1} for PM, 1MM, and 2MM, respectively. The inset shows the best-fit Langmuir and Sips isotherms over a 10-fold wider concentration range (up to 5 μM). Error bars are calculated as in Figure 2.

of mismatched DNA and that a model that includes heterogeneity (more than a single binding energy), such as the Sips adsorption isotherm,[48,49] is necessary. In fact, the Sips model can be used to interpret the data in Figure 3, yielding binding constants that decrease with increasing degree of mismatch. These mismatched duplexes have reduced thermodynamic stability compared to perfectly matched hybrids.[21,30]

To understand how erroneous conclusions can be drawn from binding isotherm results, we must examine the models and the fitting procedures in more detail. The equilibrium binding constant for duplex formation, K_A, is obtained from the best fit to experimental binding isotherms. These are measurements of the bound target coverage, Γ_{target}, for a series of solution concentrations, c, at a fixed temperature on the same probe film. In the ideal Langmuir model where all probe sites are energetically equivalent, independent and available for binding, the measured saturation level for target binding should be equal to the coverage of immobilized probe molecules, Γ_{max}. In principle, isotherms analyzed with a Langmuir model can then be fit with a single fitting parameter, K_A. In practice, however, Γ_{max} is often an additional fitting parameter or is arbitrarily set equal to highest measured target coverage. In this study, we have an independent measurement of Γ_{max} because we determine the number of probe molecules immobilized

$$\Gamma_{target} = \Gamma_{max} \frac{(K_A \cdot c)^a}{1 + (K_A \cdot c)^a} \quad (1)$$

Note that the Sips model, eq 1, reduces to the well-known Langmuir model in the limit where $a = 1$. The exponent, a, is a parameter that represents a pseudo-Gaussian distribution of binding energies of set width. When $a = 1$, the binding energy has a single value and the equation describes a homogeneous Langmuir adsorption; if $a \neq 1$, the equation describes a heterogeneous adsorption isotherm where the degree of heterogeneity (distribution of binding energies) increases as the value of a decreases. Alternative heterogeneous isotherm models (such as second-order Langmuir) may also fit the data in Figure 3. However, the Sips model was selected because it is simple and has physically meaningful parameters that may help in our understanding of the nature of interactions present in mismatched DNA hybridization at surfaces.

Upon initial inspection of Figure 3, both the Langmuir model (solid lines) and Sips model (dashed lines) appear to fit the data equally well, given the error bars in the measurements. However, the Langmuir model (solid lines), provides a reasonably good fit only for a limited concentration range up to 400 nM, see inset, and Γ_{max} must be set to a different saturation value (100%, 70%, and 50% for PM, 1MM, and 2MM respectively) for each target in order to fit the data. The binding constants, K_A, derived from the best-fit Langmuir isotherms have the same value, $\sim 6 \times 10^7$ M^{-1}, for all three targets, inconsistent with other measurements of duplex thermodynamic stability. In contrast, the Sips model can fit the data for all three targets over a broader concentration range, up to 1 μM target (dashed lines), with physically reasonable parameters. The value of Γ_{max} is 100% for all targets and the Sips fitting parameter, a, decreases from 1.00 to 0.50 to 0.38 as the degree of mismatch increases. The corresponding values for the binding constants, K_A, decrease with increasing mismatch content as expected (6×10^7 M^{-1}, 1×10^7 M^{-1} and 2×10^6 M^{-1} for PM, 1MM, and 2MM respectively). Although this trend in thermodynamic stability is gratifying, our rejection of the Langmuir model did not assume a prior knowledge of the relative binding stability for mismatched DNA.

Although it is difficult to make direct comparisons with the literature because of differences in attachment chemistry and limited availability of probe density data, results from other laboratories are in general agreement with our binding constant values. Using SPR measurements, Corn and co-workers[50] report $K_A = 1.8 \times 10^7$ M^{-1} for a perfectly matched 18-mer DNA oligonucleotide duplex on a gold substrate, while Nielsen and co-workers[51] report $K_A = 4 \times 10^7$ M^{-1} for 15-mers attached to a dextran matrix. In addition, differences in hybridization levels have been observed for matched and mismatched targets. For example, QCM measurements find no change in the extent of hybridization when the PM target concentration varies from 500 nM to 2 μM but observe increasing binding for a MM target in the same concentration range,[42] in general agreement with our results, Figure 3 inset.

In general, DNA surface equilibrium constants appear to be depressed relative to solution, indicating a trend in the overall de-stabilization of the oligonucleotide duplexes on the surface. The stabilities of the studied surface immobilized probe-target duplexes have the same relative ranking as the analogous solution-phase duplexes, however, direct comparison of surface and solution equilibrium binding constants remains difficult because of large differences in DNA concentration and effective ionic strength in these two environments.

(48) Sips, R. *J. Chem. Phys.* **1948**, *16*, 490−495.
(49) Vijayendran, R. A.; Leckband, D. E. *Anal. Chem.* **2001**, *73*, 471−480.
(50) Nelson, B. P.; Grimsrud, T. E.; Liles, M. R.; Goodman, R. M.; Corn, R. M. *Anal. Chem.* **2001**, *73*, 1−7.
(51) Jensen, K. K.; Orum, H.; Nielsen, P. E.; Norden, B. *Biochem.* **1997**, *36*, 5072−5077.

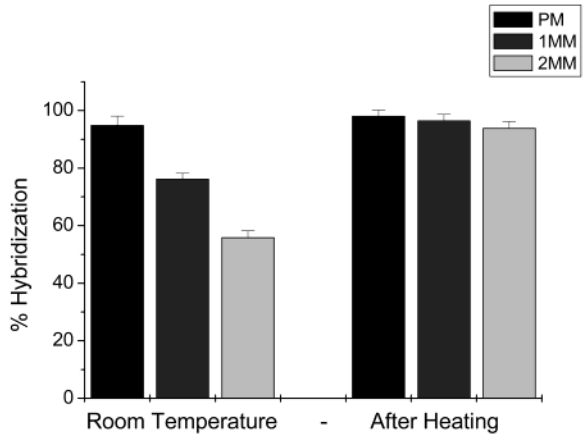

Figure 4. Comparison of the hybridization equilibrium efficiencies for PM, 1MM, 2MM with and without mild heating. The first sets of measurements, left, are done entirely under room-temperature hybridization conditions (~20 °C). The second sets of measurements, right, are taken at room temperature after heating to 37 °C in hybridization buffer for several hours.

Effect of Mild Heating. Despite the sensible trends in thermodynamic stability observed in the binding constant, maximum saturation coverage was not obtained for the mismatched targets at room temperature. To determine whether this behavior is most likely caused by an energetic barrier, we further investigated the temperature dependence of equilibrium hybridization.

The hybridization equilibrium efficiencies for the PM, 1MM, and 2MM targets were examined after mild heating and compared with room-temperature results, Figure 4. In both cases, the hybridization equilibrium efficiencies were measured after long probe-target exposure times and under the experimental conditions of 1 μM target concentration and low density (1.5×10^{12} probes/cm^2). All saturation measurements were made at room temperature for convenient comparison of hybridization efficiencies. Note that, as with all experiments discussed in this paper, the probe films were heated to ~60 °C prior to performing the first hybridization.

When duplex films, prepared previously at room temperature, were heated mildly in the hybridization buffer to 37 °C and cooled to room temperature, the equilibrium hybridization efficiencies for the mismatched targets reached nearly 100%, indicating that a different equilibrium was achieved. Thus, mild heating appears to overcome whatever energetic barrier may have prevented the mismatched targets from reaching the expected equilibrium steady state levels at room temperature. The literature for solution-phase DNA oligonucleotide duplex formation suggests that the pre-nucleation state is greatly affected by temperature, although no specific details for mismatched DNA strands are available.[13] At this time, it is not clear whether mild heating overcomes a nucleation barrier or facilitates another part of the hybridization process such as zippering, base stacking, or structural reorientation.

For 18-mer targets, 100% hybridization is observed at room temperature under saturating conditions, whereas 1 MM targets do not reach this level despite similar thermodynamic stability. Therefore, thermodynamic arguments cannot explain the lower than expected hybridization efficiency for mismatched targets under saturating conditions. Rather, there is an energetic barrier that can be overcome by mild heating, which is likely related to the structure of the mismatch targets and may depend on probe density.

Conclusion

We have investigated the effects of probe density on hybridization efficiency and kinetics for partially matched and mismatched targets. We have seen that at sufficiently low probe density, previously observed differences in the kinetics of hybridization for PM matched targets disappear. That is, at low probe density, PM targets (25 PM, 18 high, 18 low) show fast kinetics, 100% hybridization for saturating target concentrations at room temperature and exhibit binding isotherms that can be described with a simple Langmuir model. For the mismatched targets, the differences in the kinetics of hybridization also disappear at the lowest probe density, however, hybridization efficiencies do not reach expected 100% levels at room temperature and the binding isotherms are best described by a heterogeneous model, like the Sips model.

Not surprisingly, the Langmuir isotherm model, which assumes a single binding energy, could not adequately describe some of our data. A more complex heterogeneous model that allows for a distribution of binding energies was needed. Moreover, we could not simply equate the saturation coverage with the number of available binding sites, a common assumption in the analysis of binding isotherm data. Ubiquitous applications of the Langmuir model to complex binding events at interfaces and assumptions in the fitting analysis may, in some cases, call into question the reliability of binding constants determined by various techniques including SPR and fluorescence studies.

A single or double internal mismatch in a 25-nucleotide strand can dramatically alter the hybridization process, contrary to predictions of standard models of duplex formation. Our results suggest that a barrier exists for hybridization of mismatched targets, which is overcome by mild thermal heating. This barrier may arise from the complex structure of mismatched oligonucleotides or from unknown orientational or structural changes of the DNA at low probe density.

Acknowledgment. This work is supported by the NIH (CA 89562) and the NSF (DBI-0096731).

JA0279996